



ORIGIN AND DESCRIPTION OF THE MICROPORE NETWORK WITHIN THE LOWER CRETACEOUS STUART CITY TREND TIGHT- GAS LIMESTONE RESERVOIR IN PAWNEE FIELD IN SOUTH TEXAS

R. G. Loucks¹, F. J. Lucia¹, and L. E. Waite²

¹Bureau of Economic Geology, Jackson School of Geosciences,
University of Texas at Austin, Austin, Texas 78713, U.S.A.

²Pioneer Natural Resources Co., 5205 N. O'Connor Blvd., Ste. 200, Irving, Texas 75039, U.S.A.

ABSTRACT

The Stuart City Trend has been gas productive over the last 50 years. Pioneer Natural Resources Co. recently revitalized this deep, tight-gas carbonate trend by drilling numerous horizontal productive wells in Pawnee Field. The Stuart City is a shelf-edge complex showing fore reef-slope facies, thick reef-core boundstone facies, and back-reef wackestone through grainstone facies. Porosity is generally less than 8%, and permeability is less than 1 md. The major pore network consists of micropores associated with development of microrhombic calcite, which ranges between 1–6 µm in diameter. Pore-throat sizes are generally 1 µm or less. The pore network at thin-section scale shows development of micropores within grains, in grain rims, and in very fine micritic, peloidal matrix. Most macropores have been cemented by equant calcite and radial fibrous calcite. The microrhombic calcite formed by stabilization of Mg-calcite, especially in *Lithocodium-Bacinella*, foraminifera, micrite envelopes, and very fine peloids. The process of formation is by dissolution of original Mg-calcite nanocrystallites (averaging 50 to 200 nm in diameter) in allochems and carbonate mud and reprecipitation of microrhombic calcite, which shows competitive growth with other microrhombic crystals. This transformation process also increased the size of pore throats between crystals, improving permeability. In Pawnee Field, this micropore network is developed in all facies over 1000 ft of section. This field is an example of a tight-gas reservoir in which macropores are cemented during burial diagenesis and micropores, being more resistant to cementation, remain open to depths of 13,000 to 15,000 ft.

INTRODUCTION

The deeply buried Stuart City Trend limestone deposited along the Lower Cretaceous (middle Albian) paleoshelf margin in South Texas (Figs. 1 and 2) is an excellent example of a tight-gas limestone play in which permeability is generally less than 1 md and economic production depends on high-pressure, artificially stimulated horizontal wells. The Stuart City Trend has been productive for gas over the last 50 years. Pioneer Natural Resources Co. recently revitalized this deep, tight-gas trend by initiating a multiwell project of horizontal wells (Waite, 2009).

The major goal of this study was to investigate the origin of the Stuart City Trend tight-gas reservoir. Specific objectives of this paper are to (1) review reservoir development and production history of Pawnee Field; (2) describe the general depositional setting and associated facies of this shelf-margin complex;

(3) define the diagenetic history of the reservoir, emphasizing events that affected reservoir quality; and (4) discuss, in depth, the origin and description of microrhombic calcite and associated micropores that form the predominant pore network. In addressing these objectives, we hope to gain a greater understanding of the origins of the Stuart City Trend and other carbonate tight-gas reservoirs. Such knowledge is becoming more important as deeper gas reservoirs are more commonly explored.

DEVELOPMENT AND PRODUCTION HISTORY OF THE PAWNEE TREND

Pawnee Field, located in Bee and Live Oak counties, Texas (Fig. 1), is the second-largest gas field within the Stuart City Trend. As of December 2012, Pawnee Field had produced a cumulative total of 257 billion cubic ft of gas. The field has undergone significant growth over the past 15 years, which is related mostly to advances in horizontal drilling and completion technology and high average natural gas prices prior to the end of 2008.

Pawnee Field was discovered in 1961 by Shell Oil Company with the drilling and completion of the O'Neal Gas Unit No. 1 and Freddie Tomasek Gas Unit No. 1 wells. The initial well, the

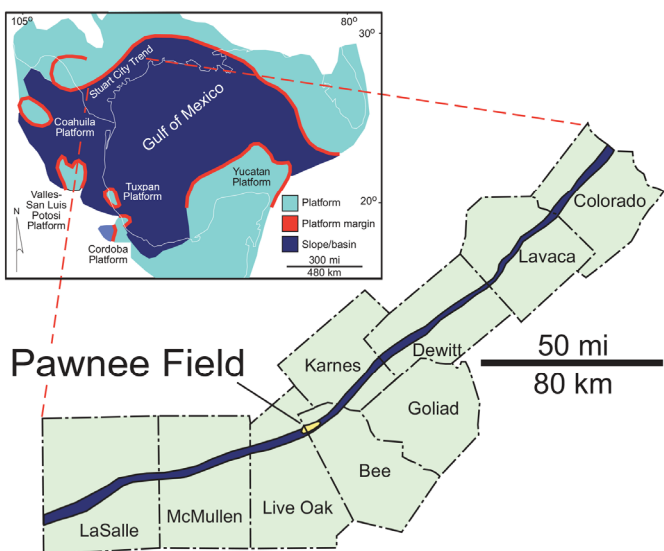


Figure 1. Location of Lower Cretaceous Stuart City Trend and Pawnee Field (modified after Bebout and Loucks, 1974; McFarlan and Menes, 1991; Waite, 2009).

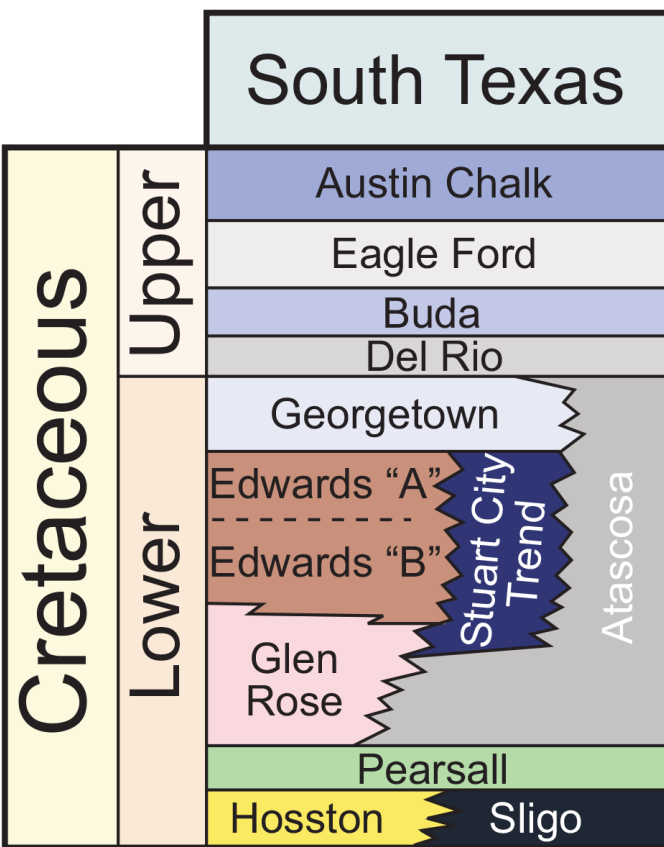


Figure 2. South Texas stratigraphic section (modified after Waite, 2009).

O’Neal No. 1, was drilled down to the Lower Cretaceous Sligo Formation at a depth of 17,000 ft, where it tested formation water. Gas was tested uphole within the Stuart City Trend limestone at depths of 13,600 to 13,900 ft, and the well was subsequently completed as a Stuart City Trend limestone producer. Shell had identified the prospect with expectations of finding

large oil reserves in a highly porous reservoir within the buried reef trend in South Texas. Despite the company’s disappointment at finding dry gas reserves in relatively low porosity and permeability reef facies, Shell subsequently drilled and completed 21 additional vertical wells during the 1960s and 70s. Shell also constructed the Pawnee gas plant, which has a processing capacity of approximately 70 million cubic ft of gas per day (MMcf/d). The existence of the gas plant was an important economic stimulus for subsequent field development.

Parker and Parsley (parent company of Pioneer Natural Resources) purchased Pawnee Field in 1986. Over the next 10 years, Pioneer Natural Resources drilled and completed a number of vertical wells within the Stuart City Trend, which increased daily field production rates to slightly greater than 5 MMcf/d. In 1999, Pioneer began an aggressive horizontal drilling program that ultimately increased field production totals to 50 MMcf/d. As of today, approximately 112 Stuart City Trend wells have been completed within the field, more than 80 of which are horizontal wells. Most horizontal wells average 3000 to 4000 ft in length and are spaced an allowable minimum of 330 ft apart. Current field limits include 15 contiguous gas units encompassing approximately 5500 acres.

METHODS AND DATA

An excellent dataset was collected from the recent drilling program by Pioneer Natural Resources, which included 3D seismic, modern wireline log suites, and cores. Some of these data have been presented in other studies, such as Waite et al. (2007) and Waite (2009), in which the regional structural and depositional setting was analyzed. Phelps (2011) and Phelps et al. (in press) completed an investigation of several cores for facies and stratigraphic architecture in order to produce a facies model, and they also analyzed the sequence stratigraphy. Missing from these studies was a detailed analysis of the diagenesis of the reservoir and associated pore network. The present study addresses both of these aspects of the reservoir.

Information collected from whole cores was the major source of data used in this study. The Pioneer National Resources No. 1 Schroeder core from Pawnee Field is our type core because, at 950 ft in length, it includes much of the Stuart City Trend section and contains abundant associated thin-section and reservoir-quality data. Thin sections from other cores in the field were also reviewed. A description of the Schroeder core is presented in Phelps (2011).

From the Schroeder core, 1262 polished thin sections were analyzed that had been impregnated with blue dye to highlight megaspores ($\sim 10 \mu\text{m}$) and with blue-fluorescent dye to highlight micropores ($\sim 10 \mu\text{m}$). They were examined to define major diagenetic features, and a selected set were point-counted (200 points) for macropore types.

Several samples were viewed using an FEI Nova NanoSEM 430 at the University of Texas at Austin. Use of this field-emission scanning electron microscope (FSEM) equipped with in-lens secondary electron detectors provided greatly increased detail of nanometer-scale features. Lower accelerating voltages (1–10 kV) were typically used on these systems to prevent beam damage, and working distances were 3 to 7 mm. Two types of samples were viewed with the FSEM: polished thin sections and rock chips. The polished thin sections were used to quantify shape and abundance of the microrhombic calcite and associated micropores. High-resolution FSEM photomicrographs were taken of selected areas for point-counting using the JMicronVision software program (Roduit, 2013). For each photograph analyzed, 2000 points were counted. Several rock chips were viewed to record the three-dimensional shape of the microrhombic calcite and associated micropores. Rock chips provided excellent photomicrographs of shape, although only qualitatively. Accurate measurements could not be made by statistical point-counting methods on chips.

Each foot of Schroeder core was analyzed for core-plug porosity and permeability analysis, and 1200 analyses were available for use. Core plugs were analyzed for porosity and permeability at both 800 and 4000 psi confining stresses. Five mercury

injection capillary pressure (MICP) analyses were obtained from the Schroeder core. Samples were analyzed up to 55,000 psi.

GENERAL DEPOSITIONAL SETTING AND LITHOFACIES REVIEW

Stuart City Trend carbonates were deposited along a relatively steep shelf margin (Phelps, 2011; Phelps et al., in press) during middle Albian time. In the United States, the margin runs from South Texas to the West Florida shelf (McFarlan and Meenes, 1991) (Fig. 1). Waite (2009) found that the primary geologic heterogeneity along the Stuart City Trend is related to deep structures controlled by faulting and salt-related tectonics. He also noted secondary influences related to position of the older Sligo shelf margin under the Stuart City Trend and to isolated block faulting along the margin.

The depositional setting and lithofacies of the Stuart City Trend have been investigated by a number of authors (e.g., Bebout and Loucks, 1974; Scott, 1990; Waite et al., 2007; Waite, 2009; Phelps et al., 2010a, 2010b, in press; Phelps, 2011). These workers all recognized the Stuart City Trend as a shelf-margin reef complex composed of a variety of facies. In general, each of the studies divides the Stuart City Trend into three general facies tracts: back reef, reef proper (reef crest and reef flat), and fore-reef/slope. Phelps (2011) and Phelps et al. (in press) presented the most detailed analysis of lithofacies and their distribution, as well as several reef-complex models to explain lithofacies distribution. In this paper only a general review of lithofacies and depositional environments is presented in order to put diagenetic and pore-type observations in perspective.

The following is a brief summary of major lithofacies assemblages of the Stuart City Trend shelf-margin complex, borrowing from the general environments presented by Bebout and Loucks (1974) and Phelps (2011). The forereef/slope lithofacies is dominated by grains that have been sourced from the shallower reef margin and includes rudist, coral, and stromatoporoid fragments. Textures include wackestones to grainstones and rudstones. Matrix varies from mud to grain rich. Phelps (2011) also noted some polymictic breccias in this facies assemblage and that the reef-wall lithofacies assemblage is bound by *Lithocodium-Bacinella* (microbialites produced by cyanobacterium (Dupraz and Strasser, 2002; Rameil et al., 2010)). Therefore, the most common textures are bindstones and framestones, with grain- to mud-dominated matrix. Organisms include calcite and siliceous sponges, stromatoporoids, corals, red algae, and foraminifera. The reef-flat lithofacies is dominated by whole and fragmented rudists. Associated grains include foraminifera, corals, red algae, and stromatoporoids. Phelps (2011) defined two boundstone types in this environment: (1) requienid bindstones containing requienids and caprinids bound by *Lithocodium-Bacinella* and (2) caprinid baffles with grain-dominated packstone matrix and containing requienids, radiolitids, and monopleurids. In the back-reef lithofacies, grain-rich textures are common, including grainstones, rudstones, and baffles. Grains include foraminifera, several rudist types, stick corals, and mollusks. As noted by Bebout and Loucks (1974) and Phelps (2011), coated grains are common in this facies. Phelps (2011) recognized the coatings as *Lithocodium-Bacinella*.

DIAGENETIC HISTORY AND PORE EVOLUTION

The diagenetic history of the Stuart City Trend limestone has been studied by several authors (e.g., Bebout and Loucks, 1974; Bebout et al., 1977; Land and Prezbindowski, 1981; Prezbindowski, 1985; Perkins, 1989). Each of these studies addresses pore networks, but only Perkins (1989) noted the development of micropores in former Mg-calcite peloidal cement as a major contributor to reservoir quality; however, he did not quantify the importance of this pore type nor its origin, nor did he comment on the contribution of micropores from the stabilization of Mg-calcite allochems.

As noted earlier in the review of lithofacies, the reef-margin complex is dominated by packstones, grainstones, rudstones, and

boundstones. In the general discussion of diagenesis that follows, a paragenetic sequence (Fig. 3) is presented that integrates observations from each of these lithofacies. This paragenetic sequence is presented for two main reasons: (1) to integrate the development of micropores into the diagenetic history of Stuart City Trend limestones and (2) to review pore evolution of Stuart City Trend limestones that transformed it into a tight-gas carbonate reservoir.

The original mineralogy of Stuart City Trend sediments was a mixture of calcite, aragonite, and Mg-calcite. Each of these mineralogies reacted differently during diagenesis (Fig. 4). Calcite remained relatively stable and did not contribute to changes in porosity. Aragonite generally completely dissolved, forming moldic pores that remained opened or filled with equant calcite. In some cases, aragonite dissolved slowly and reprecipitated along a microfront, preserving some relict texture (neomorphism of Folk, 1965). Mg-calcite followed a much more complex path, which is later presented in detail in the Origin of Microrhombic Calcite and Associated Micropores section. In general, many Mg-calcite grains, such as foraminifera, red algae, *Lithocodium-Bacinella*, micritized grains, and micrite envelopes, convert to microrhombic or microcrystalline calcite crystals ranging from less than a micrometer to 4 or 5 μm (Fig. 5). If Mg-calcite allochems convert in a relatively closed system (no large loss or gain of calcium carbonate), then a loosely packed microrhombic calcite fabric forms with associate micropores (Fig. 6). If additional calcium carbonate is added, microrhombic calcite forms, and all pores may be occluded by crystal growth (Fig. 6). Where dissolved Mg-calcite is exported from the grain, moldic pores form (Fig. 6). Other Mg-calcite allochems appear to expel magnesium, and the allochem structure is preserved.

The paragenetic sequence is divided into four diagenetic environments (Fig. 3) where major diagenetic features are described and discussed. An important factor for an understanding of observed diagenetic features in a sample is recognition of the diagenetic pathway that the original sediment followed into the

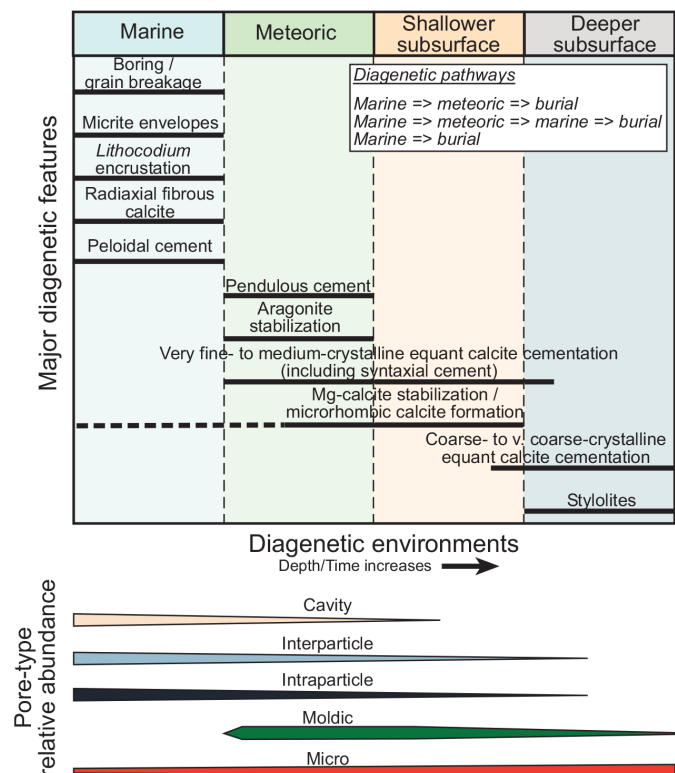


Figure 3. Paragenetic sequence chart showing major diagenetic features relative to diagenetic environments. Lower section of diagrams displays pore-type relative abundance with burial.

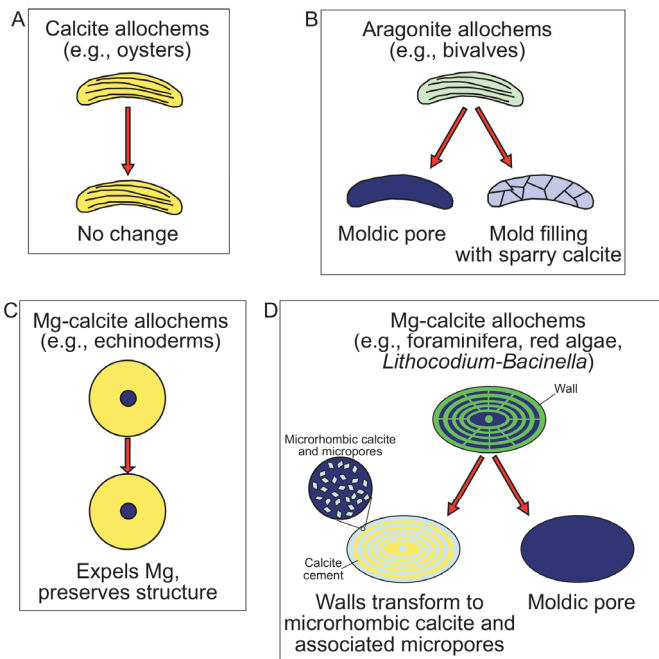


Figure 4. Schematic diagram showing general processes associated with stabilization of different mineralogies. (A) Calcite grains are relatively chemically stable and little diagenetic change occurs. (B) Aragonite is relatively chemically unstable and generally dissolves to form moldic pores. Commonly these pores are refilled with equant calcite occluding pores. (C) Mg-calcite allochems are chemically unstable; however, some Mg-calcite allochems, such as echinoderm and brachiopod allochems, appear simply to expel magnesium and retain their original structure. (D) Mg-calcite allochems, such as foraminifera, red algae, *Lithocodium-Bacinella*, transform to microrhombic calcite and associated micropores. In some cases the allochem dissolves to form moldic pores.

subsurface. All original limestone sediments in Pawnee Field were created in a marine environment, although two general pathways into the subsurface occurred. The simplest diagenetic pathway was the creation of sediment in the marine environment and burial directly into the subsurface without its being affected by meteoric waters. Another diagenetic pathway occurred when the sediment created in the marine environment was first exposed to meteoric waters before it entered the subsurface environment. A complication of this second pathway was the marine sediment being exposed to meteoric water once, then again being exposed to marine water before entering the subsurface. This later, complex pathway was documented by Bebout and Loucks (1974) for Stuart City Trend limestones.

Marine Diagenetic Environment

Several simple, but important, diagenetic events happened in this setting. Grain breakage was caused by mechanical abrasion associated with waves and currents or bioturbation abrasion that had been produced by burrowers mixing the sediment (Fig. 7A). Ease of breakage was enhanced by weakening of the shells by borings. Breakage affects porosity development by destroying intraparticle pores and producing more surface area for Mg-calcite micrite envelopes (Fig. 7A) to develop. Micrite envelopes, produced by algal and fungal borings, occur on most grains in the marine environment. They convert the outer shell layer to a thin rim of Mg-calcite cement (Windland, 1968). As discussed later in the section on development of micropores, the micrite envelope transforms to micropores and forms an important part of the effective pore network. Encrustation of grains

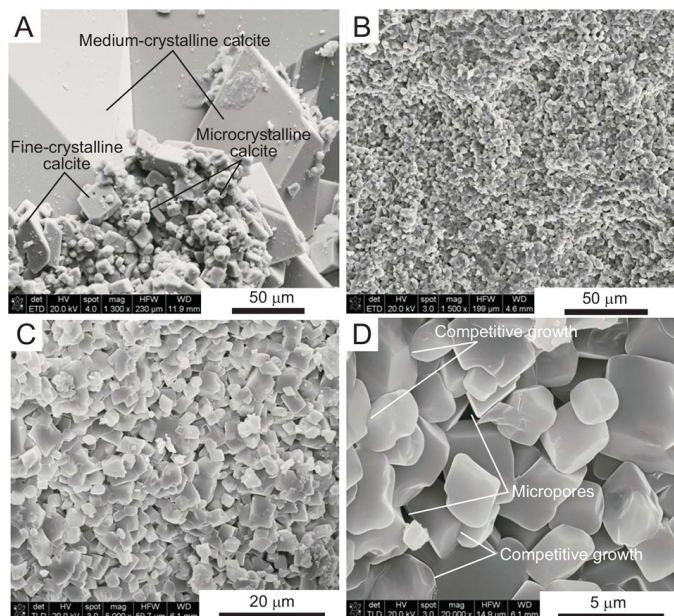


Figure 5. FSEM photomicrographs of microrhombic calcite and associated micropores. (A) Photomicrograph displaying variation in crystal sizes from microcrystalline to medium-crystalline calcite. Pioneer Schroeder No. 2 well, 13,799 ft. (B) Microcrystalline calcite, with crystal sizes ranging between 1 and 6 micrometers. Pioneer Schroeder No. 2 well, 14,056 ft. (C) Microrhombic calcite and associated micropores. Crystal size ranges between 2 and 8 micrometers. Pioneer Schroeder No. 2 well, 14,029 ft. (D) Microrhombic calcite and associated micropores. Crystals show competitive growth. Pioneer Schroeder No. 2 well, 14,029 ft.

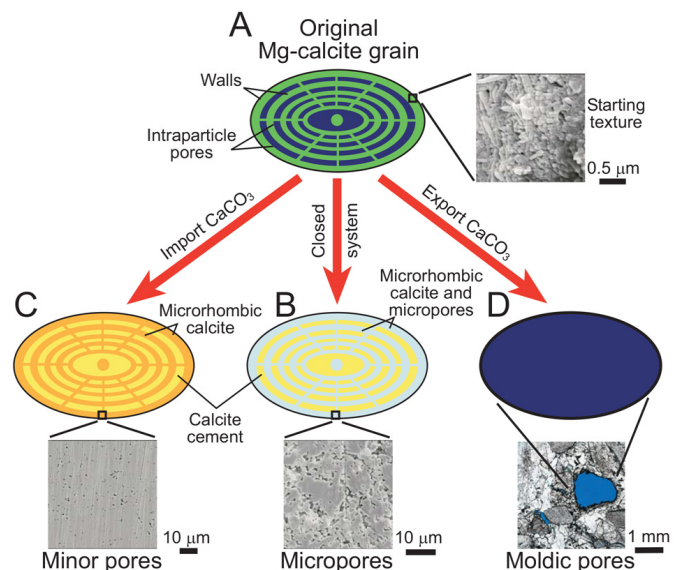


Figure 6. Schematic diagram displaying transformation of Mg-calcite to microrhombic calcite and associated micropores. (A) Original Mg-calcite grain with microtexture of rods and microcrystallites. Nanopores are between rods and crystals. (B) Transformation to microrhombic calcite in relatively closed system (allochem level) preserves porosity. (C) In a system where calcium carbonate is added to the grain, microrhombic calcite will fill nearly all pore space within the grain. (D) If abundant calcium carbonate is lost from the grain, a moldic pore will result.

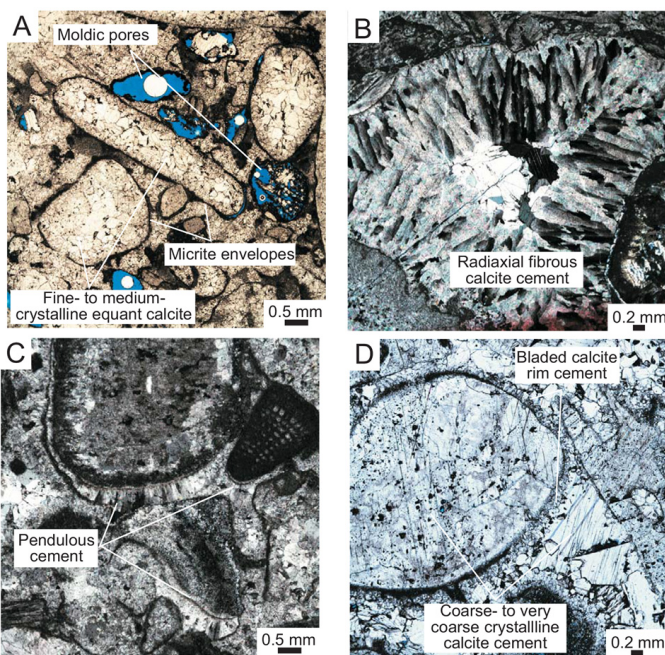


Figure 7. Thin-section photomicrographs of diagenetic features. (A) Examples of relatively tight limestone in which broken grains are preserved by micrite envelopes. Former aragonite grains are filled with fine- to medium-crystalline calcite; however, a few are preserved as moldic pores. (B) Intergranular pore partly filled with radial fibrous cement. Center of pore filled with equant calcite. Microphotograph taken with cross-polarized light. (C) Pendulous-calcite bladed cement at bottom of several grains. This cement signifies precipitation in meteoric vadose zone. Microphotograph taken with cross-polarized light. (D) Fine-crystalline bladed calcite rims several grains, and medium- to very coarse-crystalline calcite cement fills interparticle, intraparticle, and moldic pores.

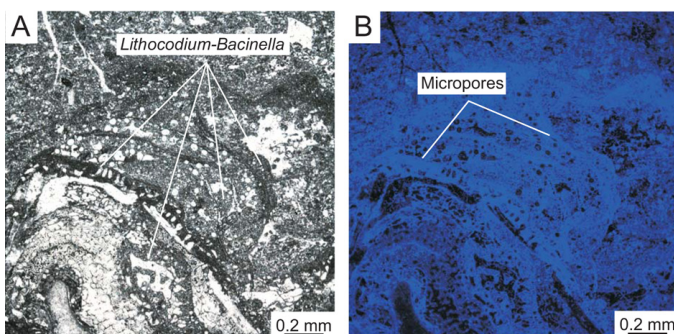


Figure 8. Photomicrographs of *Lithocodium-Bacinella* cyanobacteria. (A) Colony of *Lithocodium-Bacinella* cyanobacteria showing upward growth. (B) *Lithocodium-Bacinella*, formerly Mg-calcite, and now transformed into microrhombic calcite and associated micropores. Light-blue in photomicrograph is where blue-UV fluorescent dye penetrated micropores.

in the marine environment may bind the sediment into bindstones, or it may simply coat grains, thus enlarging them. The major encruster of the Stuart City Trend limestone is *Lithocodium-Bacinella* (Phelps, 2011; Loucks et al., 2012) (Fig. 8). *Lithocodium-Bacinella* is thought to have been composed of Mg-calcite (Loucks and Sullivan, 1987; Loucks et al., 2012) because it transforms to microrhombic calcite in a manner similar

to that of other Mg-calcite grains, such as foraminifera and red algae. Therefore, wherever *Lithocodium-Bacinella* existed, micropores formed during the transformation of Mg-calcite. *Lithocodium-Bacinella* encrustations are a major source of diagenetic micropores in all facies. Radial fibrous calcite cement is common within Stuart City Trend limestones (Bebout and Loucks, 1974; Prezbindowski, 1985) (Fig. 7B) and was documented by Prezbindowski (1985) as former Mg-calcite marine cement. This cement occludes many larger pore spaces.

Meteoric Diagenetic Environment

During sea-level lowering, Stuart City Trend sediments were exposed to meteoric waters. If subsidence was slow, the sediments may have been affected by meteoric waters more than once. Positive diagenetic evidence of exposure in the vadose zone is pendulous cement (Fig. 7C; dripstone). Bebout and Loucks (1974) described pendulous cement from Stuart City Trend grainstones. Aragonite and Mg-calcite, which were relatively stable in the marine diagenetic environment, are unstable in meteoric water (e.g., Land, 1967; Land et al., 1967). A significant product of meteoric diagenesis in Stuart City Trend limestones was the wholesale dissolution of aragonite grains (Fig. 7A). Except for the presence of micrite envelopes, the aragonite grains would have totally disappeared. Abundant moldic pores developed, some of which may have started to fill with equant calcite in the meteoric diagenetic environment or may have remained open until occluded in the shallow- to deep-burial environment (Figs. 7A and 7C). Any aragonitic mud present would also begin to stabilize in this diagenetic environment. The initial product would be a microporous mud (e.g., Steinen, 1982). Another common diagenetic product in the meteoric diagenetic environment is very fine- to medium-crystalline equant calcite cement (Figs. 7A and 7C). In Stuart City Trend limestones this is a ubiquitous cement type whose major source is the dissolution of aragonite grains. Precipitation of very fine- to medium-crystalline equant calcite cement continued into the shallow subsurface. Mg-calcite began its transformation to microrhombic calcite and associated micropores where exposed to meteoric water (Figs. 5 and 8). As mentioned earlier, details of this process are discussed in the section on the origin of microrhombic calcite and associated micropores.

Shallower Subsurface Diagenetic Environment

In sediments that were exposed to the meteoric diagenetic environment, the major processes in the shallower subsurface were the continuation of very fine- to medium-crystalline equant calcite cementation and continued Mg-calcite stabilization. In original Mg-calcite allochmes, low Mg-calcite continued to nucleate and grow. The very fine- to medium-crystalline equant calcite cement reduced porosity, and Mg-calcite stabilization ideally did not affect porosity because the process neither creates nor destroys pores but only modifies them.

In sediments that were not exposed to meteoric waters, similar diagenesis of aragonite and Mg-calcite took place, but probably at a slower rate (Knoerich and Mutti, 2003; Lucia and Loucks, 2013). Aragonite nevertheless underwent dissolution, and very fine- to medium-crystalline equant calcite cements precipitated. Also, as Mg-calcite reacted with waters out of equilibrium with its stability, microrhombic calcite and associate micropores developed. Note that no special diagenetic setting is necessary for Mg-calcite to convert to microrhombic calcite. Conversion to microrhombic calcite will take place in any fluid that is not in equilibrium with Mg-calcite (see later discussion).

Deeper Subsurface Diagenetic Environment

In the deeper diagenetic environment, two major diagenetic features were produced: coarse- to very coarse-crystalline equant calcite cementation and stylolization. The paragenetic relationship of coarse- to very coarse-crystalline equant calcite cements with other diagenetic features suggests that this cement is generally the last cement to precipitate. It tends to fill remaining pore

space (Fig. 7D). Stylolization is a product of pressure solution. Large sections of the stratigraphic section can be lost to dissolution, and the dissolved carbonate can be a major source of calcium carbonate for late cementation (Flügel, 2010, p. 320).

Pore-Evolution Summary

Initial porosity in carbonate sediments can be high and variable (40–78%; Enos and Sawatsky, 1981). In carbonate sands with equidimensional carbonate grains, porosities are similar to or higher than those of siliciclastic sands. Early carbonate muds have porosities ranging from 64 to 78% (Enos and Sawatsky, 1981). During diagenesis, these initially high porosities drop as mechanical compaction and chemical diagenesis progress.

As just noted, in the marine diagenetic environment, initial porosity of the sediment is generally high. The porosity occurs in the form of interparticle pores between grains; intraparticle pores within living cavities of biota, nanopores, and micropores within walls and tests of biota; and micropores between mud particles (Fig. 3). Two common forms of pore destruction are breakage of grains that destroys intraparticle pores and cement-filling of larger interparticle and intraparticle pores and cavities by radial fibrous calcite. Bebout and Loucks (1974) and Prezbindowski (1985) demonstrated that radial fibrous calcite occluded porosity in rudist rudstones and boundstones.

The meteoric diagenetic environment was a zone in which pores were both created and destroyed (Fig. 3). Whether porosity was enhanced or destroyed overall depended on a complex set of rock–water interactions. The major porosity production process was development of moldic pores by dissolution of aragonite grains such as caprinids, other mollusks, and corals. Even though aragonite dissolution added to porosity, the dissolved calcium carbonate was reprecipitated as very fine- to fine-crystalline equant calcite occluding abundant pores. Enhanced micropores associated with Mg-calcite stabilization began in this diagenetic environment, but ideally this process only rearranges pores within Mg-calcite grains. Carbonate sediments or poorly to moderately lithified limestones moving from this diagenetic environment into the shallow-buried subsurface diagenetic environment are estimated to have had high porosities ranging between 20 and 30%.

In the shallow-subsurface diagenetic environment, very fine- to medium-crystalline equant calcite continued to occlude interparticle, intraparticle, and moldic pores. Micropores within transforming Mg-calcite grains continued to evolve. Megapores continued to be cemented with medium- to very coarse-crystalline equant calcites into the deeper subsurface. Coarser calcite cements were the “killer” cements that occluded the last remaining megapores in the Stuart City Trend limestone, except for minor amounts of moldic pores. Micropores within the former Mg-calcite grains appear not to have been greatly affected in the deeper diagenetic realm (this concept is discussed in the next section). The final pore network in the Stuart City Trend limestone that survived into the deeper subsurface is dominated by micropores with associated rare, moldic pores (Fig. 3). This evolution of pores through burial has developed the Stuart City Trend limestone into a tight carbonate reservoir that is capable of producing gas.

Note that this burial trend of pore evolution in the Stuart City Trend limestone is similar to the pore-evolution trend seen in Tertiary sandstones in the Gulf of Mexico (Dutton and Loucks, 2010). This trend in both set of rocks follows the pattern of interparticle pores being occluded first, followed by moldic pores, and leaving micropores as the last remaining pores. In Tertiary sandstones, interparticle pores become cemented with quartz, whereas in the Stuart City Trend limestone, interparticle pores become cemented with calcite. Interparticle pores may be prone to be cemented first because they are the dominant flow path for fluids, and the outsides of crystals, such as quartz and calcite, have better nucleation sites than do the interiors of grains, such as molds in feldspars or fossil. Also, crystals growing in interparticle pores are blocked from easy entrance into moldic pores. Moldic pores do become cemented with time by interparticle crystals finding breaks in mold walls or crystal nucleating within

the mold. Micropores are probably the last pores to be cemented because they contain the smallest pore throats, thus equating to the lowest permeability and, hence, the least openness to fluid flow. Also, as discussed in the next section, larger crystals that adjoin the microporous area cannot grow into these areas. The larger crystals appear incapable of growing through the very fine pore throats and then expanding into the interior micropores. Because the larger crystals pinch out, we suggest that micropores are likely the last surviving pores in limestones that are buried deeply (see also Loucks and Sullivan, 1987).

ORIGIN OF MICRORHOMBIC CALCITE AND ASSOCIATED MICROPOROSITY

Introduction to Microrhombic Calcite and Associated Micropores

Microrhombic calcite and associated micropores were first discussed in depth at the 1987 Society of Economic Paleontologists and Mineralogists (SEPM) Midyear Meeting in Austin, Texas, in a technical session on “Reservoir Diagenesis and the Evolution of Micro- and Macro-Pore Networks in Carbonate Rocks,” convened and chaired by R. G. Loucks and C. R. Handford. In a special volume of *Sedimentary Geology* (1989) two years later, 11 papers from this session were published. Since then many authors have attempted to define the origin of microrhombic calcite and associate micropores, and the origins suggested vary greatly (Handford et al., 1989). They range from near-surface stabilization in meteoric water (e.g., Loucks and Sullivan, 1987), to stabilization during burial in marine fluids (e.g., Perkins, 1989) or evaporite-derived fluids (e.g., Cantrell and Haggerty, 1999), to deep-burial diagenesis under elevated temperature conditions (e.g., Dravis, 1989; Koepnick et al., 1994), to hydrothermal alteration (e.g., Patchen et al., 2005; Smith, 2006).

Origin hypotheses about how microrhombic calcite formed are generally based on physical paragenetic relationships and trace-element and isotope chemistry (Handford et al., 1989). The trace-element and isotope chemistry of microrhombic crystals is strong evidence for the authors that their concepts must be correct, but it is interesting to note that a similar product, microrhombic calcite, can vary quite differently chemically. Later in this section we suggest a simple explanation as to how all these authors are probably correct.

Microrhombic or microcrystalline calcite and associated micropores that form tight-gas reservoirs can be divided into three general categories: (1) coccolith-rich sediment (chalks), (2) aragonite-rich muds transformed to calcite, and (3) Mg-calcite allochems and mud (mixture of silt- and clay-size particles) transformed to calcite. Relative to Stuart City Trend limestone diagenesis and reservoir development, the third method, Mg-calcite allochems and mud transformed to calcite, is the pro-

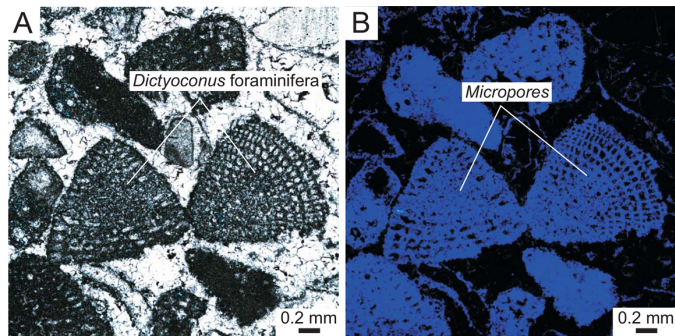


Figure 9. Photomicrographs of *Dictyoconus* showing micropores in walls. (A) *Dictyoconus* in grainstone cemented by fine- to medium-crystalline equant calcite. (B) Photomicrograph taken with blue UV light allows areas of micropores to luminesce blue.

cess responsible for the tight-gas micropore reservoir in Pawnee Field.

Definition and Description of Microrhombic Calcite and Associated Micropores in the Stuart City Trend

In the Stuart City Trend limestone, microrhombic calcite is associated with former Mg-calcite biota and carbonate mud that was probably originally a mixture of Mg-calcite and aragonite. The Mg-calcite biota that transformed to microrhombic calcite includes *Dictyoconus* and miliolid foraminifera, red algae, micritized clasts, and *Lithocodium-Bacinella*. Micrite envelopes were also Mg-calcite (Windland, 1968). A blue-fluorescent-dyed thin section of *Dictyoconus* foraminifera from the Stuart City Trend limestone was observed under plain light and mercury ultraviolet light (Fig. 9). Because the walls of the foraminifera are composed of microrhombic calcite and associated micropores, the blue-fluorescent dye highlights the wall structure.

Examples of microrhombic calcite and occurrence and quantity of micropores observed in the Stuart City Trend limestone are presented in Figures 5 and 10. Crystals range in size from 1 to 5 μm and average about 4 μm in length. The crystals are generally euhedral, but the edges may be slightly rounded. Smaller crystals ($\sim 1 \mu\text{m}$) suggest that the precursor seed for crystal growth is small ($<1 \mu\text{m}$). Competition for space between microrhombs indicates that the crystals grew outward until they were obstructed by another crystal (Fig. 5D). As discussed later, formation occurs through a dissolution/ reprecipitation process.

In any one sample, microrhombic growth varies widely in completion of growth. Some areas show a loose arrangement of microrhombs, whereas in the center of grains, the microrhombs are tightly packed and only the preservation of nm-sized interparticle pores indicates the presence of microrhombs (Figs. 11A and 11B). This arrangement of tightly packed microrhombs also suggests that microrhombic calcite is much more common than originally thought because, as it graduates to a high degree of pore filling, it can be observed only by detailed SEM observa-

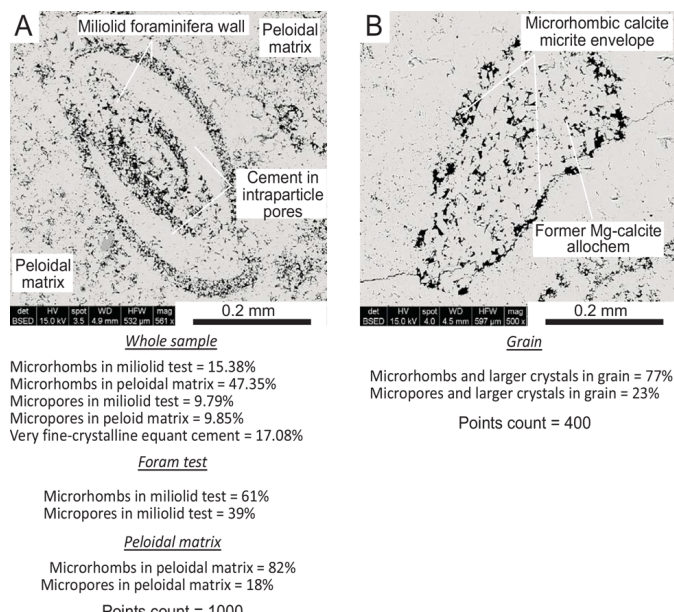


Figure 10. FSEM photomicrographs quantified for microrhombic calcite and micropores. (A) Polished thin-section backscatter image of miliolid in peloidal matrix. Both miliolid and peloidal matrix contain abundant micropores. Point-count statistics provided for sample as a whole and for foraminifera test and peloidal matrix. (B) Polished thin-section backscatter image of former Mg-calcite grain now composed of microrhombs. Original grain had a micrite envelope that now has abundant micropores. Point-count statistics provided for the grain.

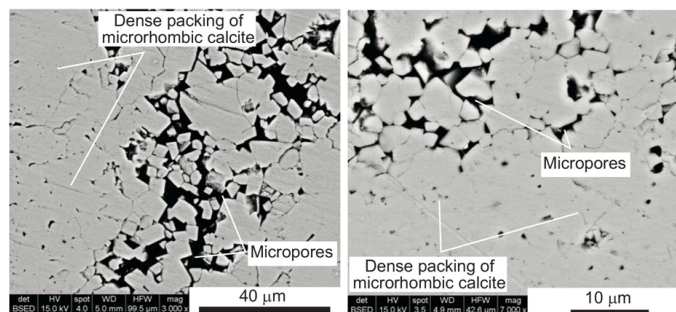


Figure 11. Backscattered photomicrograph showing microrhombic calcite distribution. Black areas are micropores. Microrhombic calcite shows varying degrees of cementation. Where crystals have competed little with other crystals, they are easy to recognize. Where they have intergrown with one another, however, they are more difficult to distinguish.

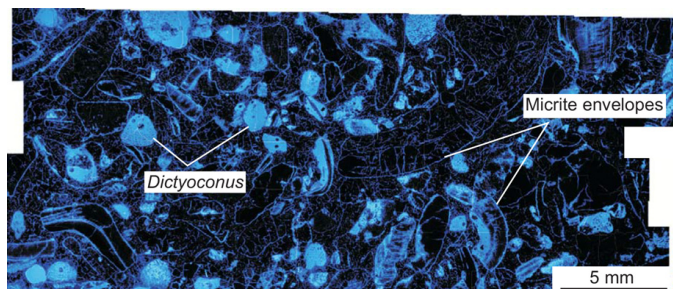


Figure 12. Mercury UV-light mosaic of photomicrographs showing micropore network (light blue) in grainstone. In this sample, micropores are predominantly in *Dictyoconus* grains and micrite envelopes. Sample depth is 13,869 ft, porosity is 7.0%, and permeability is 0.406 md.

tion. This degree of microrhombic crystal competition or growth is summarized in Figure 6 discussed earlier.

A *micropore*, as used in this study, is a pore with a long diameter less than or equal to 10 μm and/or a pore-throat diameter less than or equal to 1 μm . This definition is similar to definitions proposed by Pittman (1971), Handford et al. (1989), and Cantrell and Haggerty (1999). We also define a *micropore network* as one in which micropore throats connect the dominant pore network (Fig. 12), even if macropores are present. Note that pores should not be thought of as individual entities but as a network because this network is what controls flow or permeability.

Three-dimensional shapes of micropores can be viewed in SEM photomicrographs of rock chips (Fig. 5). For cross-sectional views of these pores, backscatter images of polished thin sections are used (Figs. 10 and 11). Pore shapes range from simple triangles to complex polyhedrons.

Origin of Stuart City Trend Microrhombic Calcite and Associated Micropores in Former Mg-Calcite Allochems

Perkins (1989) recognized microrhombic calcite and associated micropores within marine peloidal cements in Stuart City Trend limestones to the southwest of Pawnee Field. He attributed the origin of the microrhombic calcite to the alteration of Mg-calcite peloids in a closed system associated with meteoric or marine fluids. His conclusions defined only the diagenetic environment that the Mg-calcite material stabilized, however, not the actual origin of the microrhombic calcite. In order for microrhombic calcite development to be understood, original structure of the allochems needs to be investigated.

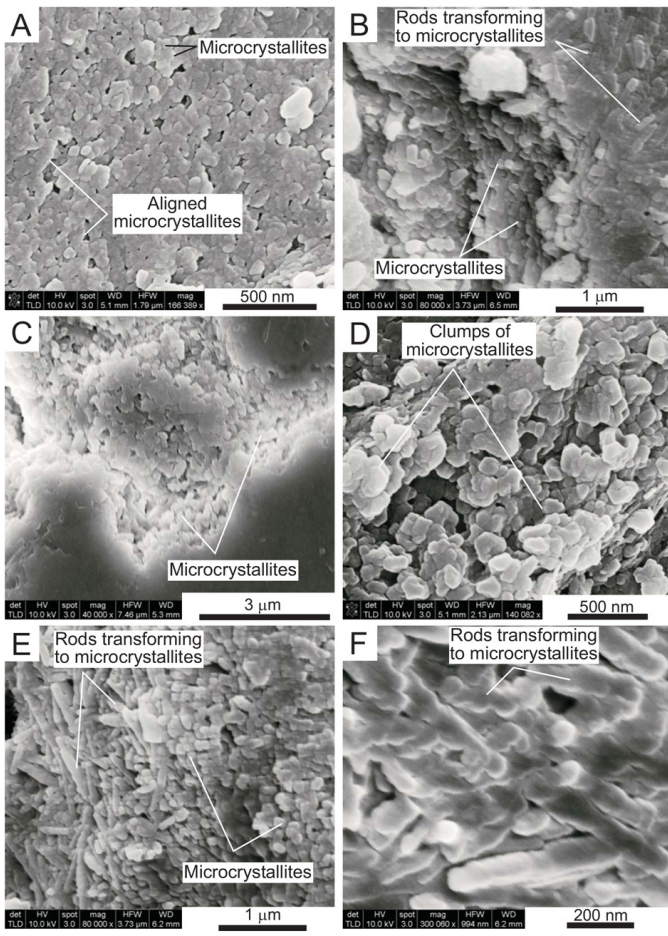


Figure 13. FSEM photomicrographs of modern Mg-calcite allochems undergoing early diagenesis to bulbous rods and microcrystallites. (A) *Goniolithon* red algae from Florida Keys showing Mg-calcite rods transforming to microcrystallites. Some microcrystallite bundles still show elongation. **(B)** *Goniolithon* red algae from Florida Keys showing Mg-calcite rods transforming to microcrystallites. Right side of photograph shows bulbous rods. **(C)** Larger foraminifera from Philippines with well-developed microcrystallites. **(D)** Larger foraminifera from Philippines with clumps of microcrystallites. **(E)** Larger foraminifera from Philippines with bulbous rods and well-developed microcrystallites. **(F)** Larger foraminifera from Philippines displaying bulbous rods.

Our approach to explaining the original wall structure of allochems consisted of selecting several modern Mg-calcite-rich allochems similar to those seen in the Stuart City Trend limestone and viewing these allochems with the FSEM. We used larger foraminifera from recent sediments in the Philippines and *Goniolithon* red algae from recent sediment in the Florida Keys. Broken pieces of skeletal material viewed under the FSEM (Fig. 13) revealed that the basic wall structure of both the larger foraminifera and red algae showed early alteration from short, several- μm -long needles to 50 to 200 nanocrystallites. This observation is similar to those Macintyre and Reid (1998) presented in their investigation of wall-structure evolution of the living foraminifera *Archaias angulatus*. They found that while the foraminifera is still alive, diagenesis begins in the older walls. In more recent parts of the foraminifera, walls consist of 2- μm -long rods of high Mg-calcite (Fig. 14A). As the walls age, these rods appear to transform to rods showing thickening in the form of nanocrystallites (Fig. 14B). In the oldest part of the walls, the rods have broken into individual nanocrystallites, with some

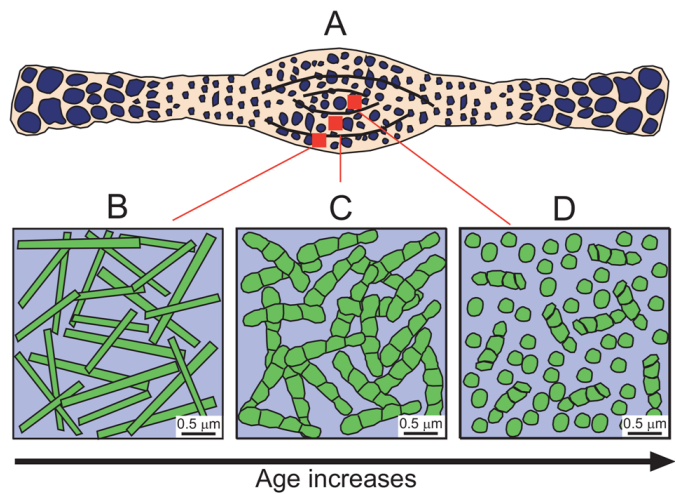


Figure 14. Schematic diagram of early diagenesis in living foraminifera. Diagram based on SEM photomicrographs from Macintyre and Reid (1998). **(A)** Drawing of cross section of recent foraminifera showing locations of drawing shown in B through D. **(B)** Youngest part of test composed of HMC rods. **(C)** Middle part of test shows initial alteration to microcrystallites approximately 100 nm in diameter. Note rods breaking into balls. **(D)** Inner or oldest part of test altered to microcrystallites.

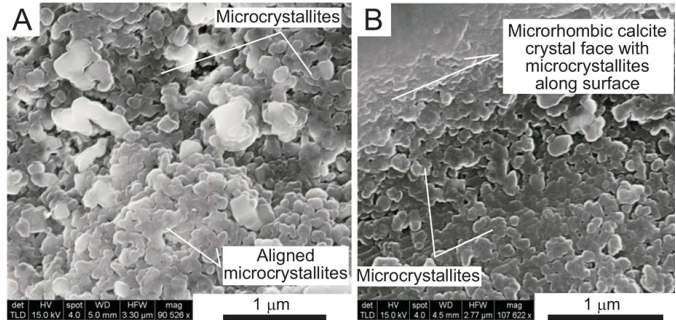


Figure 15. FSEM photomicrographs of Stuart City Trend bulbous rods and microcrystallites. (A) Schroeder 13,878-ft sample showing microcrystallites similar in size and shape to those of modern microcrystallites. **(B)** Schroeder 13,820-ft sample displaying microcrystallites. Edge of microrhomb of calcite in upper left of photomicrograph.

nanocrystallites showing alignment consistent with the precursor rods (Fig. 14D).

This discussion of modern Mg-calcite allochems demonstrates that modern foraminifera and red alga are nano- to microporous and that Mg-calcite is unstable and begins to alter early in its history. Therefore, the starting material for formation of ancient microrhombic calcite in Mg-calcite allochems seems to be a meshwork of nanocrystallites in a nano- to micropore network (Figs. 13 and 14). Evidence supporting this assumption comes from FSEM analysis of Stuart City Trend microrhombic calcite samples. In some samples, areas of what we think are original nanocrystallites are preserved (Fig. 15). Comparing modern nanocrystallites with ancient Stuart City Trend nanocrystallites shows that they are nearly identical in appearance and size. Some of the Stuart City Trend nanocrystallites even show some of the original alignment to former rods (Fig. 15).

We therefore propose a dissolution/reprecipitation process in a relatively closed system within the allochems for development of microrhombic calcite and associated micropores. Mg-calcite,

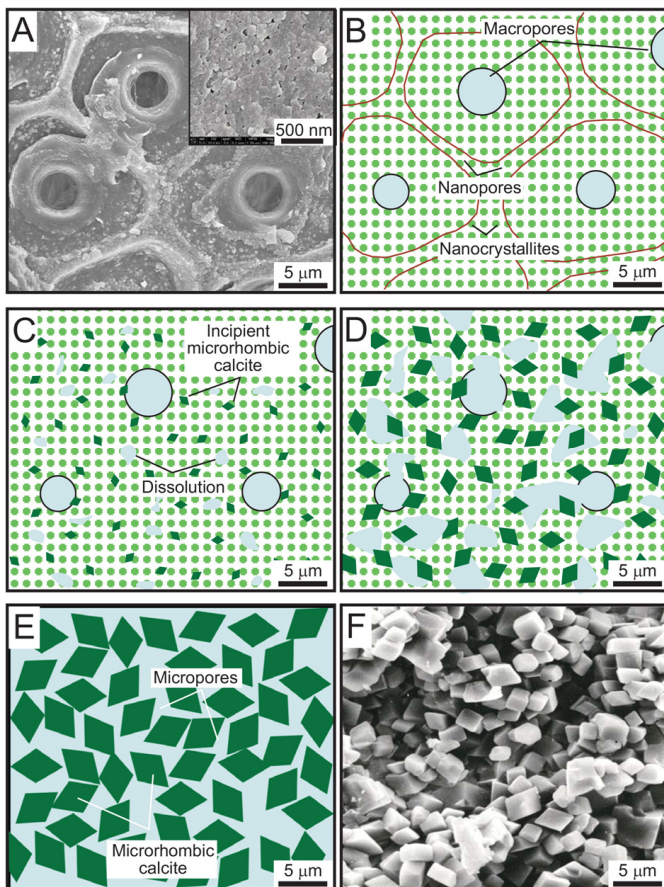


Figure 16. Schematic displaying steps in transformation of Mg-calcite to microrhombic calcite and associated micropores. (A) FSEM photomicrograph of *Goniolithon* an example of starting material. Upper right, nanostructure of modern *Goniolithon*. (B) Schematic of starting material shown in A. Dots represent nanocrystallites, and spaces between dots are nanopores. (C) Early stage of dissolution-reprecipitation. (D) Intermediate stage of dissolution-reprecipitation. (E) Final stage of complete stabilization. (F) Final microrhombic calcite fabric.

especially high Mg-calcite, is unstable, and as soon it is out of equilibrium with its original environment, it will begin to stabilize to low Mg-calcite. We envision the following process for transformation of Mg-calcite to microrhombic calcite (Fig. 16):

Stage 1: Starting material (Figs. 16A and 16B). The starting material in the marine diagenetic environment is allochems or micrite envelopes that are Mg-calcite. The structure of the original material is thought to be a meshwork of rods and nanocrystallites, as described earlier. The rods and nanocrystallites are separated by nano- to micropores.

Stage 2: Initial dissolution/reprecipitation (Fig. 16C). This stage is initiated as the unstable Mg-calcite allochems are subjected to fluids that are out of equilibrium with the allochems. It does not matter what the fluid is for the Mg-calcite allochems to start transforming to stable low Mg-calcite. During this stage some of the nanocrystallites dissolve, and other areas in the meshwork act as seed crystals. These seed areas may be small crystals of low Mg-calcite developed in the Mg-calcite meshwork. As dissolution proceeds, the calcium carbonate is transferred to the growing microrhombs.

Stage 3: Advanced dissolution/reprecipitation (Fig. 16D). As dissolution continues, the rods and nanocrystallites disappear, and the microrhombs continue to grow. Both crystals and pore spaces are enlarged.

Stage 4: Complete stabilization (Figs. 16E and 16F). The process is complete when the allochems are totally transformed

to microcrystalline calcite and associated micropores. If the allochem-scale system is a relatively closed system, porosity can be conserved, but how closed the system remains can vary.

If the allochem-scale system is not closed, porosity will not be conserved. In a system where calcium carbonate is lost, moldic pores can develop (Fig. 6). If the system incorporates more calcium carbonate, the microrhombs will continue to grow and destroy porosity (Fig. 11).

This model also explains why the studies listed earlier suggest that contrasting specific fluids for microrhombic transformation may all be correct. Unstable Mg-calcite will begin transformation as soon it is out of equilibrium, and no special or specific water chemistry is necessary to promote this disequilibrium. As the microrhombic calcite starts to grow, it incorporates the chemical signature of the fluids. Disequilibrium has promoted transformation, not the specific chemistry of the fluid. What the various fluid-chemical signatures from the literature suggest is that Mg-calcite transformation can occur in significantly different diagenetic fluids.

Origin of Stuart City Trend Microrhombic Calcite and Associated Micropores in Lime-Mud Matrix

In Stuart City Trend limestones, microrhombic calcite and associated micropores were also developed in lime-mud matrix. Identification of the original composition of lime mud is impossible because it is now transformed to low Mg-calcite. However, given the generally chemistry of Albian seas (Lowenstein et al., 2001) deposition of Mg-calcite mud would be expected, but abundant aragonite allochems were also deposited within the Stuart City Trend limestones, suggesting that some aragonite mud would be expected. Therefore, we assume that the lime-mud matrix within Stuart City Trend wackestones and packstones was a mixture of aragonite and Mg-calcite.

The mud that was Mg-calcite would have followed the same pathway as the larger Mg-calcite allochems to form microrhombic calcite and associated micropores. It is also well known that aragonite transition to low Mg-calcite will form polyhedral rhombs and associated micropores (e.g., Steinen, 1982; Lucia and Loucks, 2013). Therefore, lime-mud matrix in the packstone will add to the pore network and permeability. In contrast, the cement-filled space between grains in grainstone will be impermeable.

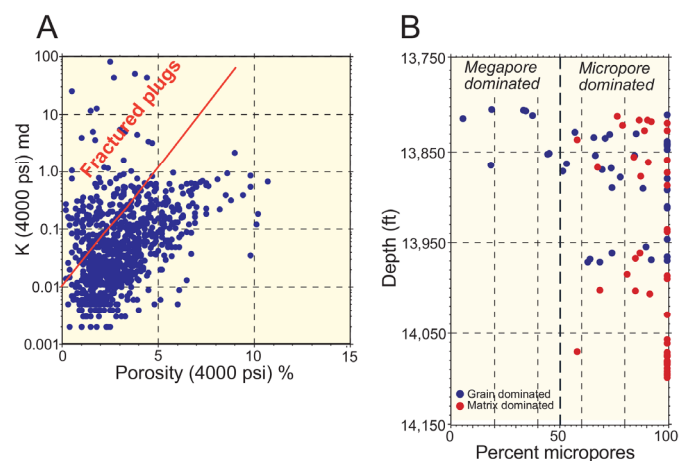


Figure 17. Reservoir quality and pore-network data. (A) Scattergram of porosity versus permeability for Schroeder core. Lower porosity-higher permeability field marked and related to fractured plugs on the basis of observation of plugs. (B) Scattergram of relative percent of micropores versus depth of top 350 ft of Schroeder core. Samples broken out by texture. Nearly all samples dominated by micropores in both grainstones and packstones. Some grainstones at top of core have moldic pores.

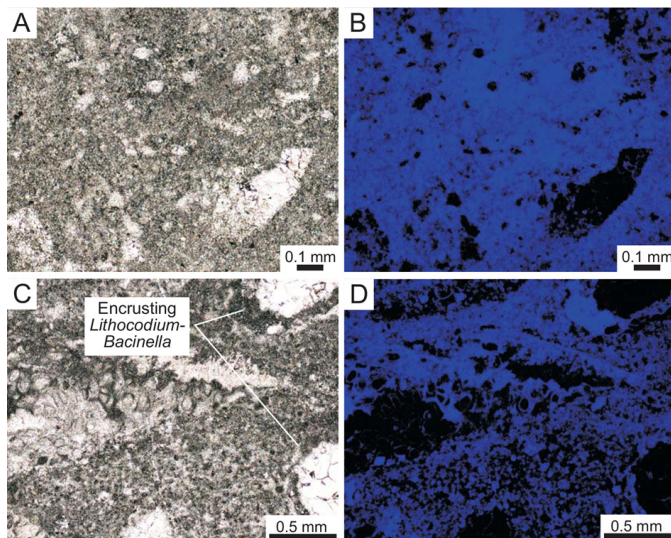


Figure 18. Examples of micropore networks in wackestones and packstones as seen in thin sections. (A) Schroeder 14,431-ft skeletal, peloidal lime wackestone. Micropores in peloidal mud matrix. (B) Same as A, but photographed in mercury UV light. Light-blue areas micropore rich. (C) Schroeder 14,390-ft encrusted skeletal lime, mud-dominated packstone. Micropores in encrusting coats and in peloidal mud matrix. (D) Same as C but photographed in mercury UV light. Light-blue areas micropore rich.

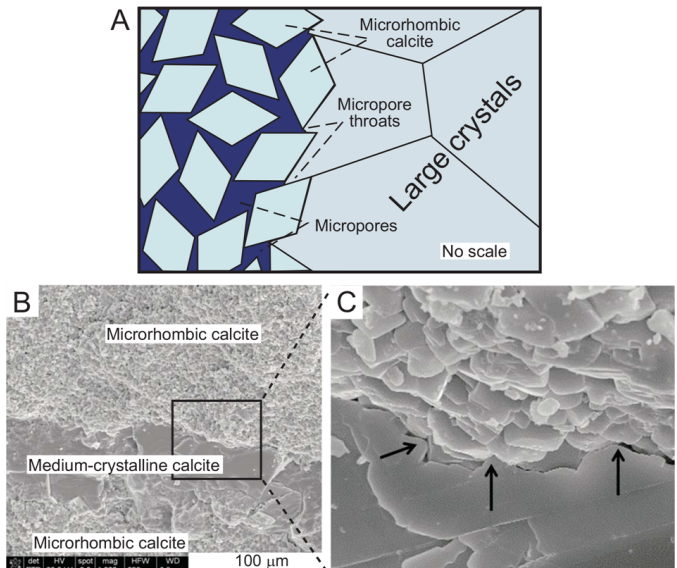


Figure 19. Explanation and evidence of larger crystals not penetrating into micropore areas. (A) Schematic diagram showing larger crystals pinching out as they grow into micropore areas. (B) FSEM photomicrograph example from Schroeder 14,056.5-ft sample showing contact between medium-crystalline calcite and microporous, microrhombic calcite areas. (C) Enlargement of B demonstrating that larger calcite crystals pinch out as they try to grow into micropore-rich area. This phenomenon promotes preservation of micropores.

STUART CITY TREND LIMESTONE TIGHT-GAS RESERVOIR PORE NETWORK

Pore Network Description

The pore network consists of two pore types—(1) moldic pores after dissolution of aragonite allochems such as bivalves and rudists and (2) micropores in allochems, micrite envelopes, and mud matrix (Figs. 7A and 12). Micropores are the dominant pore type (Figs. 12 and 17B). A cross-plot shows porosity versus permeability analyses at 4,000 psi for the Pioneer No. 1 Schroeder core (Fig. 17A). Porosity ranges between 1.5 and 8%, and permeability ranges between 0.01 and 1 md.

Micropores occur in three general positions: (1) within allochems (Figs. 9, 10, and 12), (2) in micrite envelopes (Figs. 7A and 12) and *Lithocodium* coats (Fig. 8), and within matrix (Figs. 8 and 18). The connectivity of the pore system can vary depending on whether the texture of a limestone is a grainstone, packstone, or wackestone.

In grainstones the interparticle pore network is cemented by medium- to very coarse-crystalline calcite and radial calcite. Therefore, micropores are limited to grains and rims (Fig. 12). The micropore network is connected by grain contacts, with most micropores being associated with the grains (Fig. 12). Some grainstones have a few percent of moldic pores, which, core-plug analysis shows, slightly enhance permeability.

Grains in packstone are supported, and the pore space between the grains is partly to completely filled by lime-mud matrix, some of which has a fine peloidal texture and is thought to have been high Mg-calcite mud peloids. In packstone, micropores are not associated only with grains, but also with the matrix (Figs. 18C and 18D). Therefore, the pore network or connectivity is not restricted to grain contacts because the matrix adds to connectivity. In wackestones, grains float in the mud matrix, and grain contacts are rarer than in packstones. Therefore, the major control on connectivity is through microporous matrix (Figs. 18A and 16B).

A mosaic of photomicrographs of a grainstone taken in UV light reveals the pore network or connectivity (Fig. 12). All

pores are in allochems or rims. Porosity of the sample is 7.0%, and permeability is 0.41 md.

An important observation that is substantiated by the Stuart City pore evolution is that micropores are the deepest surviving pores with depth (increasing temperature) in limestones (Loucks and Sullivan, 1987). The reason for the preservation of these pores, as suggested by Loucks and Sullivan (1987), is that these are areas of low fluid flow, so the microrhombs cease to grow and larger crystals growing next to the micropore area cannot penetrate the micropore pore throats. The larger calcite crystals grew into the outer layer of the micropore-rich area and pinched off (Fig. 19). They did not grow into the interior or the micropore area.

Dravis (1989) suggested that microrhombic calcite and associated micropores developed in the deeper-burial diagenetic realm by burial dissolution after precipitation of coarser calcite crystals. He observed that larger calcite crystals stopped at the boundary of micropore-rich areas, and he concluded that the coarser crystals had to have been precipitated first. Our observations indicate that this idea by Dravis (1989) is not a valid paragenetic relationship.

Petrophysical Analysis of Micropores

Five samples from Pawnee Field were selected, in which the rock fabrics were grain-dominated packstones and grainstones, so that the effect of micropores on permeability might be investigated. Blue-fluorescent-dyed epoxy thin sections and FSEM observations show that micropores are within micritic envelopes and grains. Because the micropores in these samples are located within grains, they are referred to as intragrain microporosity. Intragrain micropores are a type of separate vug pores (Lucia, 1995, 2007) and typically reduce permeability over what would be expected if all porosity were to be located between grains. However, values of porosity and permeability from Pawnee Field plot in the Lucia class-1 field (Lucia, 1995) instead of to the far right of the class-1 field, as predicted (Fig. 20A). Comparing Stuart City Trend micropore data with published micropore data

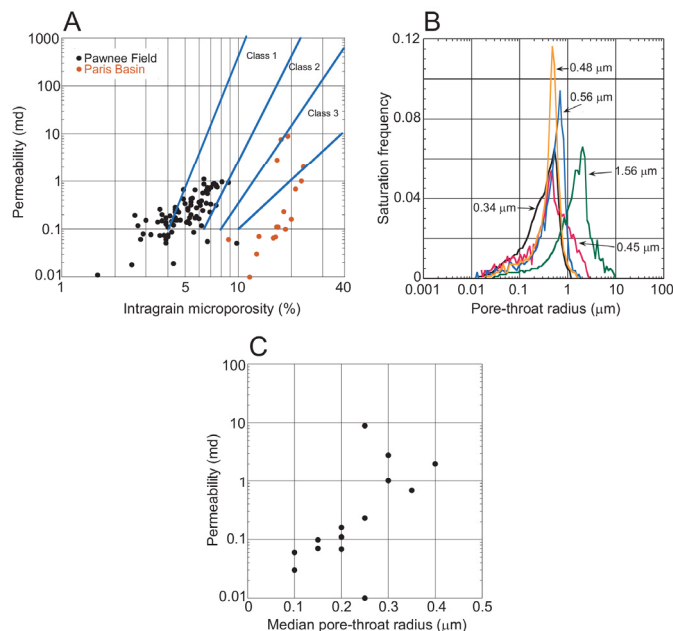


Figure 20. Petrophysical-analysis data. (A) Porosity versus permeability cross-plot with Lucia classes (Lucia, 1995) comparing data from Schroeder well in Pawnee Field with data from Paris Basin (Casteleyn et al., 2010). (B) Plot of pore-throat sizes of cemented grainstones from Schroeder well. (C) Plot of permeability versus pore-throat radius of Paris Basin data (Casteleyn et al., 2010) showing trend of increasing permeability with increasing pore-throat size.

from Cretaceous grainstones in the Paris Basin, France (Casteleyn et al., 2010) is informative. The Paris Basin limestones have intragrain microporosity and no intergrain pore space, and the core data plot to the far right of the class-1 field, as would be predicted by Lucia (1995, 2007) (Fig. 20A).

The selected sample set of grainstones from the Schroeder well were studied to investigate this anomalous petrophysical behavior. Mercury injection capillary pressure (MICP) analyses were obtained for the samples. Permeability is a function of pore-size distribution, and one measure of this parameter is pore-throat size distribution calculated from MICP data (Fig. 20B). Median pore-throat radii (PTR) range from 0.34 to 1.56 μm and average 0.68 μm. The largest PTR value has the highest permeability. Published average PTR data from 15 cemented grainstone samples from the Paris Basin (Casteleyn et al., 2010) have PTR values ranging from 0.1 to 0.35 μm and an average value of 0.22 μm. There is a general relationship between average PTR and permeability (Fig. 20C). The difference in the porosity-permeability plots between these two datasets is clearly related to the difference in PTR. Within each dataset, however, permeability appears to be related to PTR and porosity.

SEM images were prepared for the five MICP samples so that the characteristics of the micropores might be investigated. Of particular interest were the size of the microrhombic calcite crystals and the distribution of micropores within the grains. The crystal size of the four samples with the smallest PTS's is about 4 μm, and the crystal size of the sample with the largest PTS is about 6.5 μm, suggesting a relationship between PTS and crystal size. The smaller PTS in the Paris data suggests a smaller crystal size. No detailed information on crystal sizes has been published for the Paris Basin data. However, Casteleyn et al. (2010) found that micrite crystal size is less than 4 micrometers, which supports the concept that the smaller PTS in the Paris data is related to a crystal size smaller than the crystal size observed in Pawnee Field.

Therefore, the reason that cemented grainstones and grain-dominated packstones in Pawnee Field plot in the Lucia class-1 field rather than to the far right on the cross-plot in Figure 20A as

predicted is related to the larger pore-throat size. Consequently, permeability of Stuart City Trend limestones is a function of number of intragrain micropores, pore-throat size, and crystal size. In turn, predicting microrhombic crystal size is an important parameter for predicting the permeability of intragrain micropore limestones. The distribution of micropores within the grains (grain proper or micrite envelope) may have some impact on permeability as well; however, no obvious relationship was observed in this sample set.

CONCLUSIONS

Stuart City Trend Pawnee Field is a tight-gas limestone reservoir composed of micropores related to the transformation of Mg-calcite allochems and matrix to low Mg-calcite. Except for a minor number of moldic pores, micropores are the dominant pore type. This micropore network exists vertically throughout the Stuart City Trend (hundreds of feet) and laterally along the whole of the Stuart City Trend in Texas (hundreds of miles), as observed in a series of other cores. The micropore network also survives to greater burial depths than do macropores.

The formation of microrhombic calcite and associated micropores in Stuart City Trend limestones is related to the transformation of unstable Mg-calcite, and the process of transformation was by dissolution/reprecipitation. No special pore water or diagenetic environment was needed to promote this transformation. As the transformation of Mg-calcite progressed, resulting microrhombs incorporated the chemical signature of the associated fluid.

Our observations of the Stuart City Trend limestone and many other limestones throughout the world suggest that the microrhombic calcite associated with Mg-calcite stabilization is a common diagenetic product. Where it is associated with micropores, it is easy to identify, but where the microrhombs fill all the pore space within an allochem, it is more difficult to recognize.

With the advent of horizontal drilling and high-pressure hydraulic fracturing, tight-gas limestone reservoirs similar to the Stuart City Trend Pawnee reservoir are attractive targets. The observations and concepts gained from investigating the Pawnee microporous reservoir may help in an understanding of and in prediction of other, similar reservoirs at depth.

ACKNOWLEDGMENTS

This research was funded by the Carbonate Reservoir Characterization Research Laboratory at the Bureau of Economic Geology. Pioneer Natural Resources provided core and core data. Industry members include Aramco, Anadarko Petroleum Corporation, BGP (China National Petroleum Corp.), Apache, Baker Hughes, BG International, BGP, BP, BPC, Cenovus, Chevron, ConocoPhillips, Devon, ExxonMobil, Husky, JAPEX, KinderMorgan, Maersk, OXY, Petrobras, PetroChina, Pioneer, Repsol, Shell, Statoil, Suncor, and Talisman. Editing was provided by Lana Dieterich, Bureau of Economic Geology. The authors acknowledge reviews by Faith Amadi and an anonymous reviewer and by Editor Tucker F. Hentz and Associate Editor R. P. Major. Publication was authorized by the Director, Bureau of Economic Geology, Jackson School of Geosciences, University of Texas at Austin.

REFERENCES CITED

- Bebout, D. G., and R. G. Loucks, 1974, Stuart City Trend (Lower Cretaceous), South Texas—A carbonate shelf margin model for hydrocarbon exploration: Texas Bureau of Economic Geology Report of Investigations 78, Austin, 80 p.
- Bebout, D. G., R. A. Schatzinger, and R. G. Loucks, 1977, Porosity distribution in the Stuart City Trend, Lower Cretaceous, South Texas, in D. G. Bebout and R. G. Loucks, eds., Cretaceous carbonates of Texas and Mexico, applications to subsurface exploration: Texas Bureau of Economic Geology Report of Investigations 89, Austin, p. 234–256.

- Cantrell, D. L., and E. M. Hagerty, 1999, Microporosity in Arab formation carbonates, Saudi Arabia: *GeoArabia*, v. 4, p. 129–154.
- Casteleyn, L., P. Robion, P.-Y. Collin, B. Menéndez, C. David, G. Desaubliaux, N. Fernandes, R. Dreux, G. Badiner, E. Brosse, and C. Rigollet, 2010, Interrelations of the petrophysical, sedimentological and microstructural properties of the Oolithe Blanche Formation (Bathonian, saline aquifer of the Paris Basin): *Sedimentary Geology*, v. 230, p. 123–138, doi:10.1016%2Fj.sedgeo.2010.07.003.
- Dravis, J. J., 1989, Deep-burial microporosity in Upper Jurassic Haynesville oolitic grainstones, East Texas: *Sedimentary Geology*, v. 63, p. 325–341, doi:10.1016%2F0037-0738%2889%2990139-5.
- Dupraz, C., and A. Strasser, 2002, Nutritional modes in coral-microbial reefs (Jurassic, Oxfordian, Switzerland): Evolution of trophic structure as a response to environmental change: *Palaios*, v. 17, p. 449–471, doi:10.1169%2F0883-1351%282002%29017%3C0449%3ANMICMR%3E2.0.CO%3B2.
- Dutton, S. P., and R. G. Loucks, 2010, Diagenetic controls on evolution of porosity and permeability in lower Tertiary Wilcox sandstones from shallow to ultradeep (200–6700 m) burial, Gulf of Mexico Basin, U.S.A.: *Marine and Petroleum Geology*, v. 27, p. 69–81, doi:10.1016/j.marpetgeo.2009.08.008.
- Enos, P., and L. H. Sawatsky, 1981, Pore networks in Holocene carbonate sediments: *Journal of Sedimentary Research*, v. 51, p. 961–985.
- Flügel, E., 2010, Microfacies of carbonate rocks: Analysis, interpretation and application: Springer, Berlin, Germany, 984 p.
- Folk, R. L., 1965, Some aspects of recrystallization in ancient limestones, in L. C. Pray and R. C. Murray, eds., Dolomitization and limestone diagenesis—A symposium: Society of Economic Paleontologists and Mineralogists Special Publication 13, Tulsa, Oklahoma, p. 14–48.
- Handford, C. R., R. G. Loucks, and S. O. Moshier, 1989, Preface to nature and origin of microrhombic calcite and associated microporosity in carbonate strata: *Sedimentary Geology*, v. 63, p. 187–189.
- Knoerich, A. C., and M. Mutti, 2003, Controls of facies and sediment composition on the diagenetic pathway of shallow-water heterozoan carbonates: The Oligocene of the Maltese Islands: *International Journal of Earth Science*, v. 92, p. 494–510, doi:10.1007%2Fs00531-003-0329-8.
- Koepnick, R. B., L. E. Waite, G. S. Kompanik, M. J. Al-Shammary, and M. O. Al-Amoudi, 1994, Sequence stratigraphic geometries and burial-related microporosity development: Controls on performance of the Hadriya reservoir (upper Jurassic) Berri Field, Saudi Arabia, in M. I. Al-Husseini, ed., Middle East Petroleum Geosciences Conference, GEO '94, v. 2: Gulf PetroLink, Manama, Bahrain, p. 615–623.
- Land, L. S., 1967, Diagenesis of skeletal carbonates: *Journal of Sedimentary Petrology*, v. 37, p. 914–930.
- Land, L. S., F. T. MacKenzie, and S. J. Gould, 1967, Pleistocene history of Bermuda: *Geological Society of America Bulletin*, v. 79, p. 993–1006, doi:10.1130%2F0016-7606%281967%2978%5B993%3APHOB%5D2.0.CO%3B2.
- Land, L. S., and D. R. Prezbindowski, 1981, The origin and evolution of saline formation water, Lower Cretaceous carbonates, south-central Texas: *Journal of Hydrology*, v. 54, p. 51–74, doi:10.1016%2F0022-1694%2881%2990152-9.
- Loucks, R. G., F. J. Lucia, and L. Waite, 2012, Origin and distribution of microrhombic calcite and associated micropores in the Lower Cretaceous Stuart City tight-gas-carbonate play in South Texas (abs.): American Association of Petroleum Geologists, Annual Convention Abstract 1217848, 1 p.
- Loucks, R. G., and P. A. Sullivan, 1987, Microrhombic calcite diagenesis and associated microporosity in deeply buried Lower Cretaceous shelf-margin limestones: Society of Economic Paleontologists and Mineralogists Annual Midyear Meeting Abstracts, IV, p. 49–50.
- Lowenstein, T. K., M. N. Timofeeff, S. T. Brennan, L. A. Hardie, and R. V. Demicco, 2001, Oscillations in Phanerozoic seawater chemistry: Evidence from fluid inclusions: *Science*, v. 294, p. 1086–1088, doi:10.1126/science.1064280.
- Lucia, F. J., 1995, Rock-fabric/petrophysical classification of carbonate pore space for reservoir characterization: *American Association of Petroleum Geologists Bulletin*, v. 79, p. 1275–1300.
- Lucia, F. J., 2007, Carbonate reservoir characterization, 2nd ed.: Springer-Verlag, New York, New York, 336 p., doi:10.1007%2F978-3-662-03985-4.
- Lucia, F. J., and R. G. Loucks, 2013, Micropores in carbonate mud: Early development and petrophysics: *Gulf Coast Association of Geological Societies Journal*, v. 2, p. 1–10.
- Macintyre, I. G., and R. P. Reid, 1998, Recrystallization in living porcelaneous foraminifera (*Archaias angulatus*): Textural changes without mineralogic alteration: *Journal of Sedimentary Research*, v. 68, p. 11–19, doi:10.2110%2Fjsr.68.11.
- McFarlan, E., Jr., and L. S. Menes, 1991, Lower Cretaceous, in A. Salvador, ed., The geology of North America, v. J: The Gulf of Mexico Basin: Geological Society of America, Boulder, Colorado, p. 181–204.
- Patchen, D. G., L. B. Smith, R. Riey, M. Baranowski, S. Harris, H. Hickman, J. Bocan, and M. Hohn, 2005, Creating a geologic play book for Trenton–Black River Appalachian Basin exploration, <http://www.osti.gov/bridge/product.biblio.jsp?osti_id=895657> Last accessed March 10, 2012.
- Perkins, R. D., 1989, Origin of micro-rhombic calcite matrix within Cretaceous reservoir rock, West Stuart City Trend, Texas: *Sedimentary Geology*, v. 63, p. 313–321, doi:10.1016%2F0037-0738%2889%2990138-3.
- Phelps, R. M., 2011, Middle-Hauterivian to Lower-Campanian sequence stratigraphy and stable isotope geochemistry of the Comanche Platform, South Texas: Ph.D. dissertation, University of Texas at Austin, 227 p.
- Phelps, R. M., C. Kerans, and R. G. Loucks, 2010a, High-resolution regional sequence stratigraphic framework of Aptian through Coniacian strata in the Comanche Shelf, Central and South Texas: *Gulf Coast Association of Geologic Societies Transactions*, v. 60, p. 755–758.
- Phelps, R. M., C. Kerans, L. Waite, and C. Zahm, 2010b, Stuart City margin architectural variability and the effect of regional structural heterogeneity: *Gulf Coast Association of Geologic Societies Transactions*, v. 60, p. 759–763.
- Phelps, R. M., C. Kerans, R. G. Loucks, R. Da-Gama, J. Jeremiah, and D. Hull, in press, Second-order supersequences, shelf morphology, and facies distributions of the Cretaceous (Valangianian–Campanian) passive margin, northern Gulf of Mexico: *Sedimentology*.
- Pittman, E. D., 1971, Microporosity in carbonate rocks: *American Association of Petroleum Geologists Bulletin*, v. 55, p. 1873–1881.
- Prezbindowski, D. R., 1985, Burial cementation—Is it important? A case study, Stuart City Trend, south central Texas: Society of Economic Paleontologists and Mineralogists Special Publication 37, Tulsa, Oklahoma, p. 241–264.
- Ramiel, N., A. Immenhauser, G. Warrlich, H. Hillgaertner, and H. J. Droste, 2010, Morphological patterns of Aptian *Lithocodium-Bacinella* geobodies; relation to environment and scale: *Sedimentology*, v. 57, p. 883–911, doi:10.1111%2Fj.1365-3091.2009.01124.x.
- Roduit, N., 2013, JMicVision: Image analysis toolbox for measuring and quantifying components of high-definition images, version 1.2.7, <<http://www.jmicvision.com>> Accessed February 12, 2013.
- Scott, R. W., 1990, Models and stratigraphy of mid-Cretaceous reef communities, Gulf of Mexico, in B. H. Lidz, ed., Concepts in sedimentology and paleontology, v. 2: Society for Sedimentary Geology, Tulsa, Oklahoma, p. 1–99, doi:10.2110%2Fcsp.90.02.
- Smith, L. B., 2006, Hydrothermal dolomitization and leaching of carbonate reservoirs: GEO Middle East Conference and Exhibition, March 27–29, Manama, Bahrain.
- Steinen, R. P., 1982, SEM observations on the replacement of Bahaman mud by calcite: *Geology*, v. 10, p. 471–475, doi:10.

- 1130%2F0091-7613%281982%2910%3C471%3ASOOTRO%
3E2.0.CO%3B2.
- Waite, L. E., 2009, Edwards (Stuart City) shelf margin of South Texas: New data, new concepts: American Association of Petroleum Geologists Search and Discovery Article 10177, Tulsa, Oklahoma, <<http://www.searchanddiscovery.com/documents/2009/10177waite/index.htm>> Last accessed March 12, 2013.
- Waite, L. E., R. W. Scott, and C. Kerans, 2007, Middle Albian age of the regional dense marker bed in the Edwards Group, Pawnee Field, south-central Texas: Gulf Coast Association of Geologic Societies Transactions, v. 57, p. 759–774.
- Windland, A. D., 1968, The role of High Mg-calcite in the preservation of micrite envelopes and textural features of organic sediments: Journal of Sedimentary Research, v. 38, p. 1320–1325.